Soil Science Society of America Journal

TECHNICAL NOTE

Fundamental Soil Science

Measuring shrinkage of expansive soils using a novel automated high-frequency setup

B. R. Lexmond¹ B. van Dam² | C. V. Hockin³ | G. Erkens^{1,4} | J. Griffioen^{3,5} | E. Stouthamer¹

Correspondence

B. R. Lexmond, Department of Physical Geography, Utrecht University, PO Box 80.115, 3508 TC Utrecht, The Netherlands. Email: b.r.lexmond@uu.nl

Assigned to Associate Editor Ryan Stewart.

Funding information

Dutch Research Council, Grant/Award Number: NWO-NWA-ORC; Utrecht University; Wageningen University; Delft University of Technology; The Dutch Ministry of Infrastructure & Water Management; The Dutch Ministry of the Interior & Kingdom Relations; Deltares; Wageningen Environmental Research; TNO Geological Survey of The Netherlands: STOWA; Water Authority: Hoogheemraadschap de Stichtse Rijnlanden; Water Authority Drents Overijsselse Delta; Province of Utrecht; Province of Zuid-Holland: Municipality of Gouda: Platform Soft Soil; Sweco; Tauw BV; Toegepaste en Technische Wetenschappen, NWO, Grant/Award Number: NWA.1160.18.259

Abstract

Soil shrinkage characteristic curves are used to describe the shrinkage behavior and hydraulic properties of unsaturated soils. To construct soil shrinkage characteristic curves, a high-data-density measurement method is needed that relates water content to soil volume changes. We present a fully automated soil shrinkage measurement setup, based on the simplified evaporation method, to characterize the shrinkage behavior of undisturbed natural expansive clay soils. The high data density creates the opportunity to produce soil shrinkage characteristic curves without the need for a mathematical model. The technique allows for resaturation of the samples after drying, enabling differentiation between reversible and irreversible shrinkage. The setup consists of the commercialized HYPROP2 apparatus combined with optical distance sensors to measure the horizontal and vertical dimensions of the samples, yielding data on the sample volume, weight, and soil water suction. The measurement frequency is once per 10 min, and the measurement period is up to 4 weeks, providing a detailed time series of the drying and shrinkage characteristics. The setup can capture the different shrinkage phases and offers the opportunity to relate the soil shrinkage characteristic curve to soil water suction. The measurement data acquisition rate and accuracy enable detailed interpretation of soil water retention curves for nonrigid soils and are shown to be essential for understanding and quantifying the shrinkage potential of several types of deposits.

Abbreviations: CT, computed tomography; SSCC, soil shrinkage characteristic curve; SWRC, soil water retention curve.

This is an open access article under the terms of the Creative Commons Attribution-NonCommercial-NoDerivs License, which permits use and distribution in any medium, provided the original work is properly cited, the use is non-commercial and no modifications or adaptations are made.

© 2024 The Author(s). Soil Science Society of America Journal published by Wiley Periodicals LLC on behalf of Soil Science Society of America.

Soil Sci. Soc. Am. J. 2024;1–10. wileyonlinelibrary.com/journal/saj2

¹Department of Physical Geography, Utrecht University, Utrecht, The Netherlands

²Earth Simulation Lab, Utrecht University, Utrecht, The Netherlands

³TNO Geological Survey of the Netherlands, Utrecht, The Netherlands

⁴Deltares, Delft, The Netherlands

⁵Copernicus Institute of Sustainable Development, Utrecht University, Utrecht, The Netherlands

Plain Language Summary

Soil shrinkage is the decrease of soil volume due to lower water levels, which can damage infrastructure, cause land subsidence, and alter soil properties. To predict soil shrinkage accurately, it should be monitored either in the field or on natural samples in the lab, requiring high data density. We developed and tested a method to capture the shrinkage behavior of natural soil samples. Our results show that this method allows us to describe shrinkage without relying on mathematical models and also study the effects of soil wetting. This study enhances our ability to measure and understand soil shrinkage, which is crucial for predicting soil behavior in various environmental and engineering scenarios.

1 | INTRODUCTION

Soil shrinkage characteristic curves (SSCCs) are used to study the soil structure (Braudeau et al., 1999), water flow and the changes therein during drying, including related changes in the transport of colloids and smaller molecules (Beven & Germann, 1982; Crescimanno & Provenzano, 1999), and shrinkage itself. SSCCs are also needed to construct soil water retention curves (SWRCs) for nonrigid soils (Boivin et al., 2006; Saha & Sekharan, 2021), as the pore size distribution changes during shrinkage and swelling (Yan et al., 2021). An SSCC relates the specific volume or void ratio to the water content, under free external stress conditions, during drying. The curves show up to four phases—structural shrinkage, proportional shrinkage, residual shrinkage, and zero shrinkage—depending on the sample composition (Peng & Horn, 2007). Structural shrinkage is only identified in structured soils (Peng & Horn, 2013) and indicates the drying of large interaggregate pores and channels (Cornelis et al., 2006). These pores empty without considerable reduction of the total bulk soil volume due to the relatively low suction and interparticle stresses (Lu & Dong, 2017). The proportional shrinkage occurs in saturated conditions (with the exception of large interaggregate pores), and the void ratio loss is proportional to the water loss. The residual shrinkage starts after air entry, and the slope of the SSC decreases gradually during this phase until it flattens, at which point the zero shrinkage phase begins. During the last phase, the void ratio remains unchanged during continued water loss.

The choice of sample preparation and measurement technique to create SSCCs depends on the sample type and objective of the study. Many techniques do not allow for resaturation of samples due to resin coating of samples and therefore should not be applied when expecting reversible and irreversible shrinkage. When studying shrinkage and swelling, it is necessary to discern between reversible and irreversible shrinkage to assess future vulnerability to land movement or subsidence. Therefore, a measurement tech-

nique should allow for resaturation after soil shrinkage measurements, such as using rubber sample rings (Schindler et al., 2015). When using a technique that does not allow to describe internal volume changes (e.g., not a computed tomography [CT]), desiccation cracks within the samples should be prevented to be able to measure the actual bulk volume change. The easiest option is to minimize moisture gradients and the buildup of tensile stresses, by keeping the evaporation rate low (Peron et al., 2009). This lengthens the measurement duration but creates the opportunity to have frequent measurements of the shrinkage behavior.

Measuring SSCCs and SWRCs has proven to be a time-consuming task. Braudeau et al. (1999) stated the need for continuous measurements of volume and moisture content loss to construct accurate SSCCs. However, many accurate soil shrinkage measurement techniques (Lu & Dong, 2017; Gupt et al., 2022; Lu & Kaya, 2013) are not developed to measure continuously or at a high frequency, due to the expense (CT) or long processing times. Finally, when measuring shrinkage, natural undisturbed samples should be utilized when the objective is to predict the in situ behavior, as the bulk density and soil structure are governing factors in the shrinkage characteristics (Mitchell, 1993; Peng & Horn, 2005), but other factors such as land use (Dörner et al., 2009), drying history (Basma et al., 1996), and chemical changes (Xing & Ma, 2017) influence the shrinkage too.

In this paper, we present a fully automated measurement setup that is built to describe the shrinkage behavior using the simple evaporation of undisturbed natural soil samples and analyze the results. The shrinkage is induced by evaporation, and the sample dimensions are measured frequently using optical distance sensors, in combination with measurements of the soil weight and soil water suction, utilizing the HYPROP2 apparatus in a similar way as Schindler et al. (2015). The room temperature and humidity are controlled to limit the rate of evaporation and prevent desiccation cracking. After drying, the samples are resaturated to distinguish between reversible and irreversible shrinkage, expressed as a

percentage of the original sample volume. The setup is presented alongside data analysis of three natural undisturbed samples.

2 | METHODOLOGY

2.1 | Experimental setup

The experimental setup consisted of three HYPROP2 devices (METER Group) that measured soil water suction and the weight of the samples every 10 min. In the setup, only one tensiometer per HYPROP2 was used instead of two. The HYPROP2 devices are designed to be operated with two tensiometers, but the shrinking samples bent the tensiometer shafts together and eventually broke them. The shrinkage of the sample was determined by measuring the distance to samples using five optical distance sensors (Baumer FADK 14U4470/S14/IO; specifications highlighted in Supplementary Information S1), with a beam diameter of 8 mm, every 10 min. The distance to the sample could be determined with an accuracy of 10 µm, using a CR1000 datalogger (Campbell Scientific). The optical distance sensors were installed on a mounting arm, attached to a pan/tilt head (Supplementary Information S2). The pan/tilt head, controlled via the datalogger, moved the mounting arm and sensors along the three HYPROP2 measurement setups. The sensors monitored the samples at five different locations per sample. Three sensors (1-3) were used to measure the distance to the top of the samples, and the other two sensors (4–5) measured the distance to the side of the sample (Figure 1A). The distance between the beams of the sensors was 14 mm for sensors 1–3 and 21.5 mm for sensors 4 and 5 (a detailed overview is shown in Supplementary Information S3). Reference platforms were installed in between the samples to make sure the setup was stable and to provide a reference for the sample height (Figure 1B). The setup was installed in a climate-controlled room maintained at 18°C and 60% humidity (Supplementary Information S4). These settings were determined by trial and error for these specific samples. During measurements, no artificial light was used in the climate-controlled room, so as to not influence the measurements with the optical distance sensors.

2.2 | Experimental procedure

Three natural samples were extracted from the shallow subsurface—two of them at a depth of 0.8 m below the surface, and one at 1.5 m—using a ring soil sampling set (Sample ring kit 0784SC, Ø 84 mm, Eijkelkamp Soil & Water B.V.) to minimize disturbance. The rings were either pushed or hammered into the subsurface. The rings containing the samples were sealed airtight and stored at 7°C for 4–6 weeks. Before starting the shrinkage experiments, the samples were satu-

Core Ideas

- We present a new fully automated setup to accurately measure soil shrinkage curves of expansive soils.
- The method enables the construction of soil shrinkage curves without applying a mathematical model.
- Establishing soil water retention curves can be improved by simultaneously measuring shrinkage during drying.

rated with groundwater extracted at the sample site in glass desiccators, for a period of 3 weeks. The samples were saturated via the bottom of the samples, with the water level reaching a height of 1 cm below the top of the samples. After saturation, the samples were removed from the stainless-steel rings. Samples A and B could be removed by lifting the ring, and the samples stayed on the saturation plates due to gravity. Sample C needed to be gently pushed out of the ring by hand. No deformation was observed by measuring with a digital caliper before and after removing the steel rings. To prevent evaporation on the sides of the samples, the samples were enwrapped in rubber membranes, made from rubber gloves, following the method described by Schindler et al. (2015). We measured no radial deformation after transferring the samples.

After transferring the samples, a small hole was drilled at the bottom of the samples using a small hand auger with a diameter of 5.3 mm to fit the tensiometer. The tensiometer was inserted 1.25 cm into the sample. The unused second HYPROP2 sensor hole was sealed using tape (Supplementary Information S5). The HYPROP2s were mounted on the samples to minimize handling the samples. Carefully holding the sample, the HYPROP2-mounted sample could be turned the right way up, without deforming the sample.

The samples' tops were uncovered as the measurement was started. The weight, soil water suction, height, and diameter of three samples were measured every 10 min. The height (n = 15) and diameter (n = 10) of the samples were measured at five distinct locations per sample (Supplementary Information S6), as the robotic arm moved the optical distance sensors along the samples. Measuring the different locations on the separate samples took about 1.5 min per sample. The five distinct locations were set for the total duration of the experiments and were positioned such that the beams between the locations did not overlap. The complete shrinkage measurements took 2-4 weeks to be completed. The measurements were terminated when no change in both average height and diameter was measured for 24 h. During the automated measurements of Samples A and B, manual measurements of the dimensions were also carried out using a digital caliper to

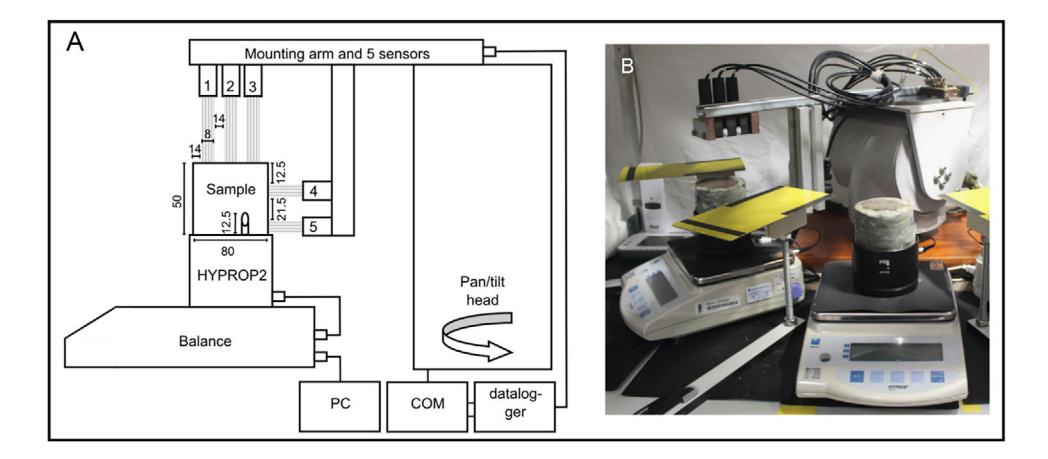


FIGURE 1 (A) Schematic overview of the measurement setup in which one out of three HYPROP2s and balances are shown. The dimensions are noted down in millimeters. The beam diameters of sensors 1–5 are all 8 mm; the distance between sensors 1–2 and 2–3 is 14 mm. The sample dimensions are the dimensions at the onset of the experiment. The COM is the communication box used to control the pan/tilt head via the datalogger. (B) Photo of the actual measurement setup including yellow reference tables. The mounting arm and sensors move in an arc over the samples and pause five times at different locations above one sample.

validate the results produced by the automated measurement method.

2.3 | Data processing

Before and after the automated measurements, sample dimensions were measured using a digital caliper as a reference to the optical distance sensor measurements. The data collected with the optical distance sensors were processed by determining the average height and diameter of the measurement points that were situated on the sample. The number of height measurements used to calculate the average decreased during the measurement series as the surface area of the sample shrunk and some measurement points fell outside the sample. A sudden increase in the standard deviation was used as an indication that a measurement point was no longer completely located on the sample surface, and from that moment onward, the point was no longer taken into account for the height averaging. The decreasing number of values did not affect the average height or diameter. Both the height and radius measurements were smoothed over time using a moving average of 12 values (2 h, based on the measurements every 10 min, selected based on trial and error) to construct smooth and insightful SSCCs, especially as both the volume and weight change diminished near the end of the experiment, yielding more noise as a result of the capacity of the data logger. To determine the volume of the sample, a truncated cone shape was assumed. The volume was thus calculated as

Volume sample =
$$\frac{1}{3}h\pi \left(r_{\text{low}}^2 + r_{\text{high}}^2 + r_{\text{low}} \times r_{\text{high}}\right)$$
,

where h is the average height (mm), $r_{\rm high}$ is the average radius (mm) at the top of the sample, and $r_{\rm low}$ is the average radius (mm) at the bottom of the sample.

The gravimetric water content was defined by weighing and oven-drying a third of each of the samples at 60°C for 24 h to prevent the oxidation of organic matter (Dexter & Richard, 2009) after the drying experiment. The remainder of the sample was used to determine sample characteristics such as particle size distribution and Atterberg limits. Water volume within the sample was derived from the weight change of the samples in combination with the density of the water, based on the known temperature of the sample (HYPROP2 internal thermometer) and the oven-dried weight of the sample.

The soil water suction was measured up to a pF value of 3.1 using the HYPROP2 tensiometers (pF = $log_{10}(lcmH_2Ol)$). Using the LABROS SoilView Analysis software (METER Group), the increasing suction was extrapolated up to the air entry point of the tensiometers (pF 3.9), using the tangent of the measured pF values (Schindler et al., 2010). The pF value between 3.1 and 6.8 was predicted based on the PDI Van Genuchten Mualem 1 – 1/n (VGM) approach (Iden & Durner, 2014; Peters, 2013, 2014) using the LABROS soil analysis software by fitting measured gravimetric water content and pF values to the retention model (Supplementary Information S7). The software offers the opportunity to use several soil hydraulic models, and we found that the model used fits our data best. The Young-Laplace equation was used to relate the measured suction to capillary radii (at the measured temperature, ignoring soil type).

The pF values can be translated to capillary pore diameters based on the Young–Laplacian equation. A pF value of 0 translates to a capillary diameter of 3000 μ m, and an increase of 1 in the pF value results in a capillary diameter that is a

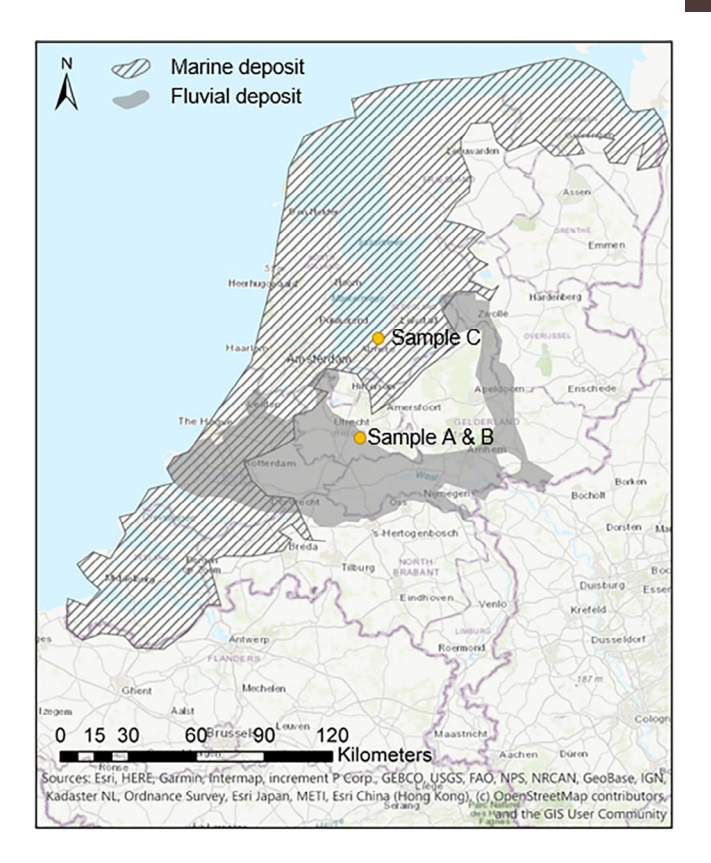


FIGURE 2 The sample locations in relation to the areas covered by Holocene clay-rich deposits in the Netherlands (Stouthamer et al., 2015).

factor of 10 smaller. Macropores are mostly defined as pores with a radius larger than 30 μ m (Mendes & Marinho, 2020) or 75 μ m (Brewer, 1964; Zaffar & Lu, 2015). These pore sizes are the ones that are stated to be responsible for structural shrinkage, the first shrinkage phase (Lu & Dong, 2017).

2.4 | Materials

To illustrate the results acquired with the setup, three samples (Table 1) are discussed. All samples are from the Netherlands and extracted from the saturated zone. Samples A and B are Holocene fluvial clay deposits, whereas Sample C is a Holocene marine silt-rich clay deposit, which was sampled in a marsh (Figure 2).

3 | RESULTS AND DISCUSSION

The soil water suction was measured from zero up to a pF value of 3.1 for all three samples, spanning 8–10 days (Figure 3). The soil water suction was measured until the cavitation point (METER Group, 2023; Schindler et al., 2010). After the air entry point was reached, the tensiometers cavitated, yielding a measured value of 0. A decrease in sample

Sample properties of Samples A, B (fluvial deposit from 0.8 m below surface), and C (marine deposit from 1.5 m below surface). TABLE

					Organic matter			
	Sampling	Saturated bulk	Specific gravity	Sand:silt:clay ^a	content (wt% of dry	Liquid limit θ	Plastic limit θ	Predrying porosity
Sample	depth (m)	density (g/cm ³)	(g/g)	(wt% of solids)	sample)	(g/g)	(g/g)	(cm^3/cm^3)
А	1.5	1.59	2.54	0.5:77.0:22.5	8.6	0.85	0.33	0.67
В	1.5	1.52	2.56	0.5:77.0:22.5	9.2	0.85	0.33	0.70
C	0.8	1.37	2.54	1.9:78.6:19.5	9.0	0.88	0.45	0.79

Vote: The specific gravity was determined using a He-pycnometer, the particle size distribution using a Malvern Mastersizer 2000 particle sizer, the organic matter content by thermogravimetric analysis, and the liquid limit with the fall cone technique

Clay <4 µm; silt <62 µm; sand <2000 µm (but only up to 500 µm was identified)

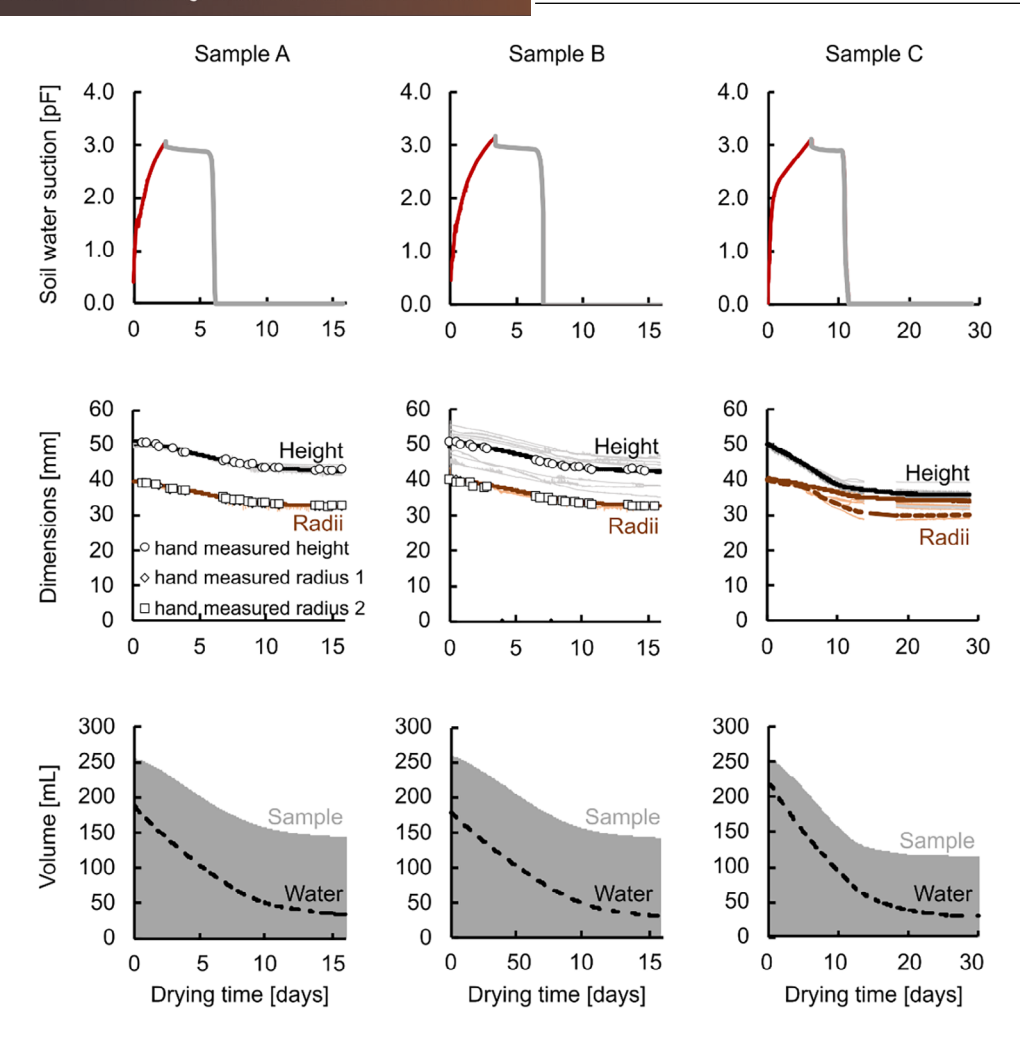


FIGURE 3 The measurement data obtained during the drying of the samples: the first row shows the regular measured soil water suction up to a pF of 3.14 (red), the limit of the tensiometers. The sudden drop to zero indicates air entering the tensiometer shafts. The gray line indicates the measured soil water suction during the boiling delay, cavitation, and air entry phases. The boiling delay phase or vapor pressure stage occurs due to boiling in the tensiometer (Schindler et al., 2010). The middle row shows the measured sample dimensions as lines, accompanied by average height and radii in bold lines. The top and bottom radii did not deviate from each other during drying in Samples A and B but did for Sample C: the radius of the top of the sample is shown as a dashed line. Data were lost during the shrinkage measurement of Sample C (Supplementary Information S8), for which the average values have been interpolated. Note that Sample C was exposed to a more extensive drying period, the horizontal axes of the plots are not the same, and no hand measurements were carried out for Sample C.

dimensions was observed in the measurements up to 15.8 days for Samples A and B and 20 days for Sample C. The separate height and radii measurements (Figure 3) showed a continuous decrease in the sample height. For Samples A and B, no offset between the top and bottom radii of the samples was identified. However, the surface of Sample B was significantly rougher than Sample A, as is visible from the larger difference between the separate height measurements for Sample B. The volume of Samples A, B, and C was 143, 141, and 107 mL, respectively, after drying for 15.8 days. Sample C showed different behavior from the other two: the increase of the soil water suction was slower than for the other samples, but the final sample volume was 101 mL after 20 days (Figure 3).

The soil shrinkage curves presented (Figure 4) allow for the identification of several shrinkage phases, based on inflection points in the curves: structural, residual, and zero shrink-

age (indicated by S, R, and Z in Figure 4). Proportional shrinkage was not identified, as a linear loss of void ratio, which is indicated as the maximum shrinkage phase (M in Figure 4). The shrinkage behavior of Samples A and B is similar, whereas Sample C showed a more extensive maximum shrinkage phase.

The SWRC constructed for Sample A was applied to the gravimetric water content evolution during the drying experiment (Figure 5A) and compared to the shrinkage rate (Figure 5B; i.e., Shrinkage rate = (Volume loss per 10 min)/(Water volume loss per 10 min)) and the normalized shrinkage rate (Figure 5C; i.e., Normalized shrinkage rate = (Volume loss per 10 min)/(Initial volume)).

The shrinkage rate (Figure 5B) and normalized soil shrinkage (Figure 5C) increased during the first 3.5 days of drying. The maximum normalized shrinkage occurred after 3.5 days

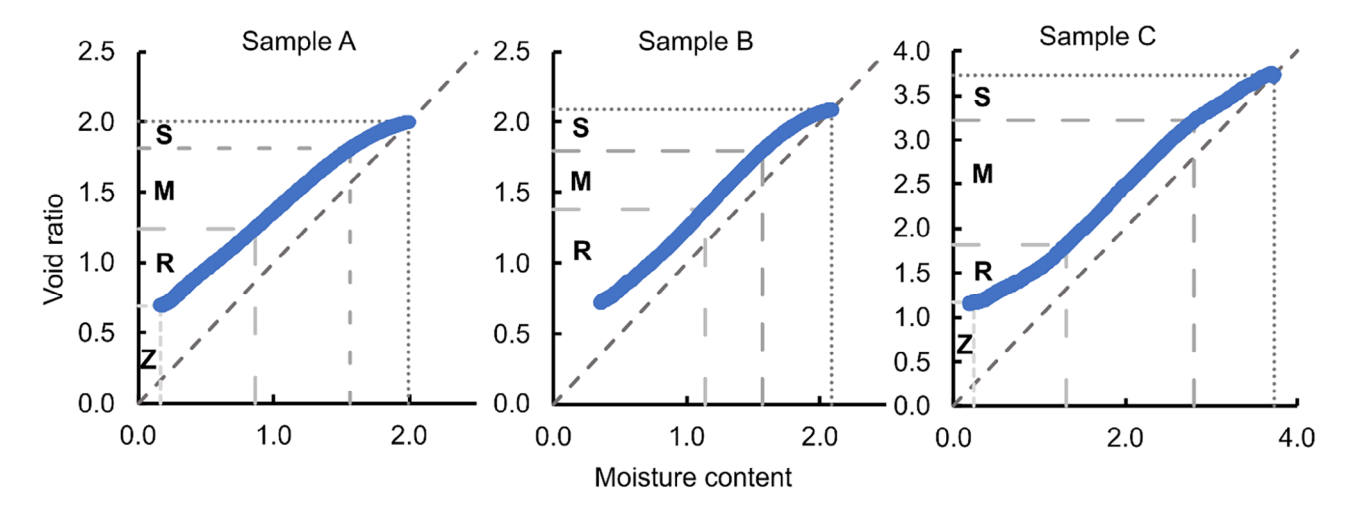


FIGURE 4 The soil shrinkage curves of Samples A, B, and C. The moisture content is defined as the volume of water in the sample over the volume of solids, whereas the void ratio represents the volume of voids over the volume of solids. The shrinkage phases are indicated in the graphs as follows: structural (S), maximum (M), residual (R), and zero (Z). Note the difference in the axes of Sample C, compared to Samples A and B.

at an extrapolated pF value of 3.5, corresponding to a capillary diameter of 0.5 μ m. Thereafter, the normalized soil shrinkage decreased, whereas the shrinkage rate remained stable until the end of Day 5, with an extrapolated pF value of 3.9–4.3, indicating a decrease in the evaporation rate and thus water loss over time. This indicates the highest shrinkage rate for capillary diameters occurs between 0.5 and 0.15 μ m, based on the extrapolated pF values between 3.5 and 3.9–4.3.

From Day 6 on, the shrinkage rate declined as the residual shrinkage phase started (Figure 5B). The largest amount of shrinkage occurred during the first 6 days, up to a pF value of 4.6 (capillary diameter of 0.08 μ m). Yan et al. (2021) found changes in the pore size distribution during swelling in a similar range for compacted London Clay. This indicates a capillary pore size range sensitive to shrinkage and swelling for nonrigid deposits.

The accuracy of the method with regard to the sample dimensions is highlighted in Figure 5B. The increase in the number of outliers during the drying process can be attributed to both the increase in surface roughness during shrinkage (Figure 3) and the reduced evaporation rate relative to a constant measurement error resulting in increasingly greater outliers when dividing the volume loss by the water weight loss. This results in greater outliers when dividing the volume loss by the measured water weight loss of the sample. Further limitations of the setup are touched upon in Supplementary Information S9.

Proportional shrinkage in which the void ratio loss equals water content loss was not identified in the soil shrinkage curves of the samples. However, there was a maximum shrinkage phase identified for all samples in which there occurred an almost linear decrease of void ratio, compared to the volumetric water content. The maximum shrinkage phase was close to proportional shrinkage as is shown in Figure 5B. The

soil water suction increase at the bottom is lagged compared to that at the top of the sample (METER Group, 2023). Therefore, the sample as a whole was not in the same shrinkage phase, yielding the lack of a proportional shrinkage phase. However, the maximum shrinkage phase is highly likely to indicate the proportional shrinkage phase in most of the samples.

After drying, the samples were fully saturated over the course of 6 weeks. Samples A and B regained 86% of the volume measured at the onset of the drying phase, indicating irreversible shrinkage was 14% of the original volume. In contrast, the reversible shrinkage accounted for 29.3% and 30.2% for Samples A and B, respectively. However, Sample C shrunk 45% irreversibly and 15% reversibly. The sample consisted of more silt than clay, compared to the other samples, explaining the lower reversible shrinkage, as the relative amount of active clay minerals is lower (Boivin et al., 2004). The higher irreversible shrinkage is explained by the different histories of the sample areas. Sample C is from an area that was drained roughly 60 years ago, while the other samples are from an area whose surface has been exposed for roughly 800 years (Stouthamer et al., 2015).

4 | CONCLUSION

The aim of this study was to construct a fully automated measurement setup to characterize soil shrinkage curves of natural and undisturbed clay samples. The drying and shrinkage behavior of the same-site fluvial samples (A and B) is akin. In contrast, the marine clay sample (C) shows more structural and proportional shrinkage compared to the other two samples and loses more volume in total. These results indicate the suitability of the newly developed measurement setup to

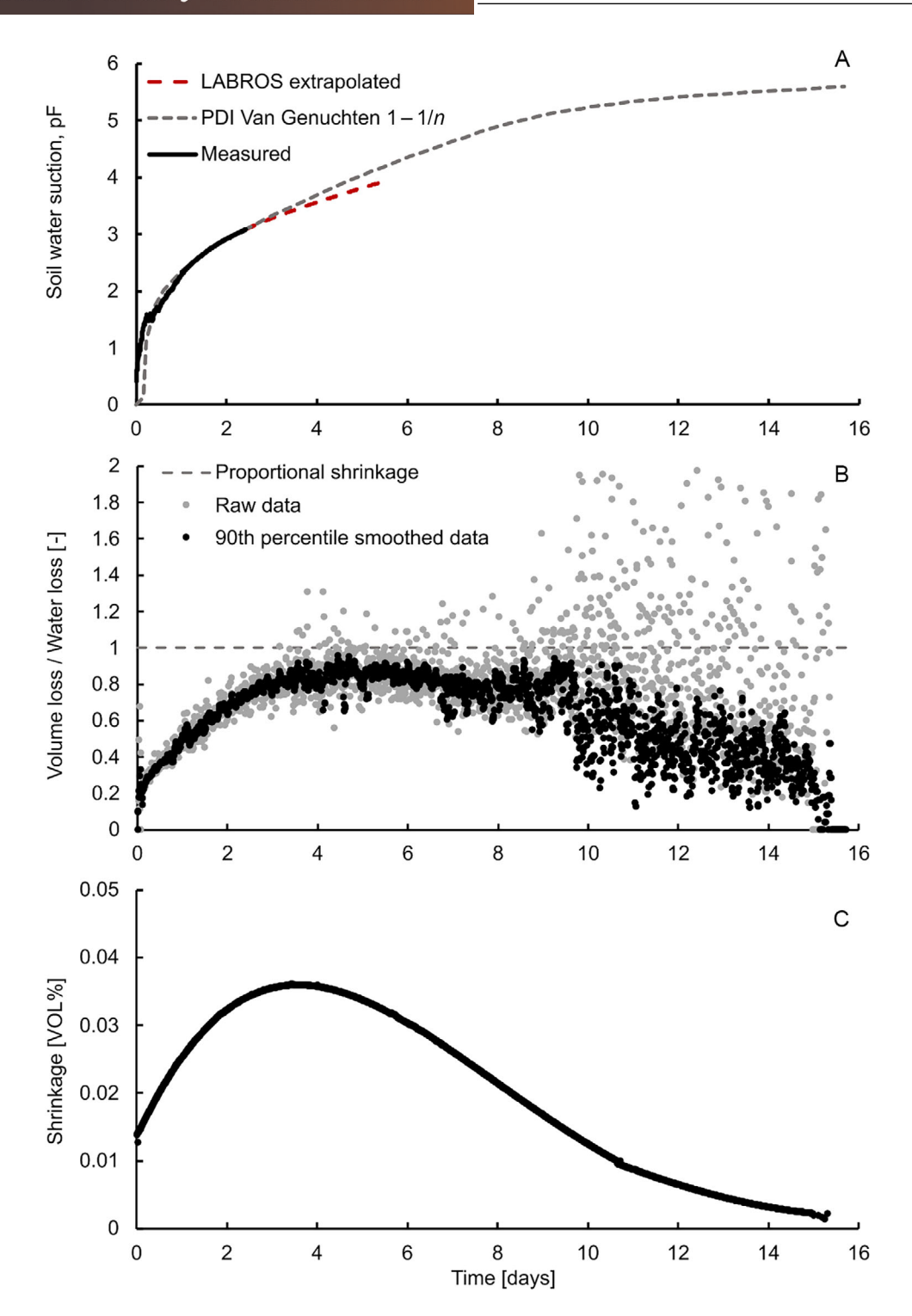


FIGURE 5 (A) The measured and extrapolated pF values of Sample A in time, at a height of 1.25 cm in the sample. The LABROS extrapolation is based on the air entry value of the tensiometers, whereas the PDI Van Genuchten 1 - 1/n extrapolation is based on fitting the model to the gravimetric water content and measured pF values. (B) The bulk volume loss per 10 min over the volumetric water loss per 10 min, both the raw data and the 90th percentile smoothed (moving average over 2 h). (C) The normalized shrinkage as the volumetric shrinkage or bulk volume loss per 10 min over the initial bulk volume.

determine the soil shrinkage as per SSCC for natural, undisturbed soil samples. The high data density allows us to determine the different shrinkage phases and the inflection points in the curves, without the need for a mathematical model to describe the shrinkage characteristics, as is a common procedure (Boivin et al., 2006; Braudeau et al., 1999; Cornelis et al., 2006; Peng & Horn, 2005). No a priori assumptions thus are needed, which is advantageous.

The method can be used to define true SWRCs (corrected for volume loss) that can be used to model water transport within shrinking or swelling soils more accurately. By combining the shrinkage measurements with SWRCs, it is possible to understand both the mechanical behavior of the soil and the transport of moisture in complex natural soft soils.

AUTHOR CONTRIBUTIONS

Bente Lexmond: Conceptualization; investigation; administration; visualization; methodology; project writing—original draft; writing—review and editing. Bas van Dam: Conceptualization; methodology; software; writing—review and editing. Cjestmir Hockin: Conceptualization; methodology; writing—review editing. Gilles Erkens: Conceptualization; funding acquisition; resources; supervision; writing—review and editing. Jasper Griffioen: Conceptualization; funding acquisition; resources; supervision; writing—review and editing. Esther Stouthamer: Conceptualization; funding acquisition; resources; supervision; writing—review and editing.

ACKNOWLEDGMENTS

The research is part of and funded by the project Living on Soft Soils: Subsidence and Society (grant no. NWA.1160.18.259). We would also like to express our gratitude to Prof. Dr. Wolfgang Durner for helping to improve the manuscript and providing additional insights into the fitting of soil water retention models. We also like to thank Marc Nijboer who contributed to the conceptual testing phase of this work.

DATA AVAILABILITY STATEMENT

The data used are available upon request from the corresponding author.

ORCID

B. R. Lexmond https://orcid.org/0000-0001-8235-5398

REFERENCES

Basma, A. A., Al-Homoud, A. S., Malkawi, A. I. H., & Al-Bashabsheh, M. A. (1996). Swelling-shrinkage behavior of natural expansive clays. *Applied Clay Science*, 11(2-4), 211–227. https://doi.org/10. 1016/S0169-1317(96)00009-9

- Beven, K., & Germann, P. (1982). Macropores and water flow in soils. *Water Resources Research*, 18(5), 1311–1325. https://doi.org/10.1029/WR018i005p01311
- Boivin, P., Garnier, P., & Tessier, D. (2004). Relationship between clay content, clay type, and shrinkage properties of soil samples. Soil Science Society of America Journal, 68(4), 1145–1153. https://doi.org/ 10.2136/sssaj2004.1145
- Boivin, P., Garnier, P., & Vauclin, M. (2006). Modeling the soil shrinkage and water retention curves with the same equations. *Soil Science Society of America Journal*, 70(4), 1082–1093. https://doi.org/10.2136/sssai2005.0218
- Braudeau, E., Costantini, J. M., Bellier, G., & Colleuille, H. (1999). New device and method for soil shrinkage curve measurement and characterization. *Soil Science Society of America Journal*, *63*(3), 525–535. https://doi.org/10.2136/sssaj1999.03615995006300030015x
- Brewer, R. (1964). Fabric and mineral analysis of soils. John Wiley & Sons.
- Cornelis, W. M., Corluy, J., Medina, H., Diaz, J., Hartmann, R., Van Meirvenne, M., & Ruiz, M. E. (2006). Measuring and modelling the soil shrinkage characteristic curve. *Geoderma*, 137(1-2), 179–191. https://doi.org/10.1016/j.geoderma.2006.08.022
- Crescimanno, G., & Provenzano, G. (1999). Soil shrinkage characteristic curve in clay soils: Measurement and prediction. *Soil Science Society of America Journal*, *63*, 25–32. https://doi.org/10.2136/sssaj1999.03615995006300010005x
- Dexter, A. R., & Richard, G. (2009). Water potentials produced by ovendrying of soil samples. Soil Science Society of America Journal, 73, 1646–1651. https://doi.org/10.2136/sssaj2008.0294N
- Dörner, J., Dec, D., Peng, X., & Horn, R. (2009). Change of shrinkage behavior of an Andisol in southern Chile: Effects of land use and wetting/drying cycles. *Soil and Tillage Research*, 106(1), 45–53. https://doi.org/10.1016/j.still.2009.09.013
- Gupt, C. B., Prakash, A., Hazra, B., & Sreedeep, S. (2022). Predictive model for soil shrinkage characteristic curve of high plastic soils. *Geotechnical Testing Journal*, 45, 101–124. https://doi.org/10.1520/ GTJ20190180
- Iden, S. C., & Durner, W. (2014). Comment on 'Simple consistent models for water retention and hydraulic conductivity in the complete moisture range' by A. Peters. Water Resources Research, 50(9), 7530–7534. https://doi.org/10.1002/2014WR015937
- Lu, N., & Dong, Y. (2017). Correlation between soil-shrinkage curve and water-retention characteristics. *Journal of Geotechnical and Geoen*vironmental Engineering, 143(9), Article 04017054. https://doi.org/ 10.1061/(ASCE)GT.1943-5606.0001741
- Lu, N., & Kaya, M. (2013). A drying cake method for measuring suctionstress characteristic curve, soil-water-retention curve, and hydraulic conductivity function. *Geotechnical Testing Journal*, 36(1), Article 20120097. https://doi.org/10.1520/GTJ20120097
- Mendes, R. M., & Marinho, F. A. M. (2020). Soil water retention curves for residual soils using traditional methods and MIP. *Geotechnical and Geological Engineering*, *38*, 5167–5177. https://doi.org/10.1007/s10706-020-01354-x
- METER Group Gmbh. (2023). *HYPROP 2 manual*. https://library.metergroup.com/Manuals/18263_HYPROP_Manual_Web.pdf
- Mitchell, J. K. (1993). Fundamentals of soil behavior. John Wiley and Sons
- Peng, X., & Horn, R. (2005). Modeling soil shrinkage curve across a wide range of soil types. *Soil Science Society of America Journal*, 69(3), 584–592. https://doi.org/10.2136/sssaj2004.0146

- Peng, X., & Horn, R. (2007). Anisotropic shrinkage and swelling of some organic and inorganic soils. *European Journal of Soil Science*, 58(1), 98–107. https://doi.org/10.1111/j.1365-2389.2006.00808.x
- Peng, X., & Horn, R. (2013). Identifying six types of soil shrinkage curves from a large set of experimental data. Soil Science Society of America Journal, 77(2), 372–381. https://doi.org/10.2136/sssaj2011. 0422
- Peron, H., Hueckel, T., Laloui, L., & Hu, L. (2009). Fundamentals of desiccation cracking of fine-grained soils: Experimental characterisation and mechanisms identification. *Canadian Geotechnical Journal*, 46(10), 1177–1201. https://doi.org/10.1139/T09-054
- Peters, A. (2013). Simple consistent models for water retention and hydraulic conductivity in the complete moisture range. *Water Resources Research*, 49(10), 6765–6780. https://doi.org/10.1002/wrcr.20548
- Peters, A. (2014). Reply to comment by S. Iden and W. Durner on "Simple consistent models for water retention and hydraulic conductivity in the complete moisture range". *Water Resources Research*, *50*(9), 7535–7539. https://doi.org/10.1002/2014WR016107
- Peters, A., Iden, S. C., & Durner, W. (2015). Revisiting the simplified evaporation method: Identification of hydraulic functions considering vapor, film and corner flow. *Journal of Hydrology*, *527*, 531–542. https://doi.org/10.1016/j.jhydrol.2015.05.020
- Saha, A., & Sekharan, S. (2021). Importance of volumetric shrinkage curve (VSC) for determination of soil–water retention curve (SWRC) for low plastic natural soils. *Journal of Hydrology*, 596, Article 126113. https://doi.org/10.1016/j.jhydrol.2021.126113
- Schindler, U. (1980). Ein Schnellverfahren zur Messung der Wasserleitfähigkeit im teilgesättigten Boden an Stechzylinderproben. *Archiv für Acker- und Pflanzenbau und Bodenkunde*, 24(1), 1–7.
- Schindler, U., Doerner, J., & Mueller, L. (2015). Simplified method for quantifying the hydraulic properties of shrinking soils. *Journal of Plant Nutrition and Soil Science*, 178(1), 136–145. https://doi.org/10. 1002/jpln.201300556

- Schindler, U., Durner, W., von Unold, G., Mueller, L., & Wieland, R. (2010). The evaporation method Extending the measurement range of soil hydraulic properties using the air-entry pressure of the ceramic cup. *Journal of Plant Nutrition and Soil Science*, 173(4), 563–572. https://doi.org/10.1002/jpln200900210
- Stouthamer, E., Cohen, K. M., & Hoek, W. Z. (2015). De vorming van het land: Geologie en geomorfologie (7th ed.). Perspectief Uitgevers.
- Xing, X., & Ma, X. (2017). Differences in loam water retention and shrinkage behavior: Effects of various types and concentrations of salt ions. Soil and Tillage Research, 167, 61–72. https://doi.org/10.1016/ i.still.2016.11.005
- Yan, W., Birle, E., & Cudmani, R. (2021). A simple approach for predicting soil water characteristic curve of clayey soils using pore size distribution data. MATEC Web of Conferences, 337(4), Article 02012.
- Zaffar, M., & Lu, S.-G. (2015). Pore size distribution of clayey soils and its correlation with soil organic matter. *Pedosphere*, 25(2), 240–249. https://doi.org/10.1016/S1002-0160(15)60009-1

SUPPORTING INFORMATION

Additional supporting information can be found online in the Supporting Information section at the end of this article.

How to cite this article: Lexmond, B. R., van Dam, B., Hockin, C. V., Erkens, G., Griffioen, J., & Stouthamer, E. (2024). Measuring shrinkage of expansive soils using a novel automated high-frequency setup. *Soil Science Society of America Journal*, 1–10. https://doi.org/10.1002/saj2.20755